NEW SELF-GRAVITATIONAL OSCILLATORY EIGENMODE PATTERNS OF SOLAR PLASMA WITH BOLTZMANN-DISTRIBUTED ELECTRONS

P. K. Karmakar
B. Borah
Department of Physics, Tezpur University, Napaam, Tezpur, Assam, India

Abstract

We attempt to propose a simplified theoretical model to study new stationary states of the nonlinear self-gravitational fluctuation dynamics of the solar plasma with the zero-inertia electrons against weakly nonlinear perturbation within the framework of the Jeans homogenization assumption. This is based on a bi-fluidic approach with the thermal electrons treated as the Boltzmann-distributed species. The joint effects of space-charge polarization, sheath-formation, and bi-layer plasma-boundary interaction through gravito-electrostatic interplay in a spherically symmetric geometry are considered. Applying a standard multiscale technique, a unique form of extended Korteweg-de Vries-Burger (*e*-KdVB) equation with a new self-consistent linear sink is methodologically developed. The origin of the unique sink lies in the spherically symmetric self-gravity contributed by the massive ions. A numerical shape-analysis with multi-parameter variation depicts the co-existence of two distinct classes of new eigenmode excitations. The fluctuation patterns evolve as *oscillatory soliton-like* and *oscillatory shock-like* patterns in judicious plasma conditions under the adiabatic electronic response. Their oscillations, arising due to resonant and non-resonant coupling phenomena with the background spectral components, get gradually damped out due to the sink. This scientific study allows us to conjecture that the model supports self-gravitational solitary (shock) waves having tails (fronts) composed of a sequence of slightly overlapping solitons with smoothly varying characteristic parameters. Our results are compared with the earlier theoretical model predictions, on-board multispace satellite data and spacecraft observations highlighting tentative future scopes.

Keywords: Self-gravity, Solar plasma, *e*-KdVB equation, Oscillatory eigenmodes

1 Introduction

Self-gravitating plasmas like the Sun, stars and their atmospheres are well-known to exhibit a rich spectrum of diverse nonlinear collective waves, oscillations and fluctuations [1-3]. They are naturally excited by the interplay of different internal mechanisms of nonlinearity, dispersion and dissipation [1-5]. Such effects interact with each other and get coupled in slow timescales (~normal mode timescale) to develop the saturated form of the eigenmode structures. Normally observed class of stellar nonlinear waves and eigenmodes of pronounced astrophysical significance include shocks, solitons, vortices, hybrid structures and so forth [2-12]. In fact, from historical point of view, the theory of nonlinear waves was first applied to the solar atmosphere in an attempt to explain the chromospheric and coronal heating [6]. It was assumed that the turbulent motion in the solar convective zone excites sound waves that propagate upwards. As a result of the effect of nonlinearity in the solar plasma, these waves steepen and form shocks and like structures. The wave energy dissipates in these shocks thereby heating the corona.

Many authors have reported the excitation, existence and propagation of a wide variety of nonlinear wave dynamics in a star like the Sun and its atmosphere by applying different model approaches centered on multiscale analyses [3-7]. For example, Ballai *et al*. [3-4, 7] have studied the nonlinear saturations of magnetosonic waves in presence of the Hall current perpendicular to the ambient magnetic field producing the wave dispersion. The wave dispersive effects have been compensated by the nonlinear steepening (due to fluidity) of the waves amid viscous effects. The most important dissipative mechanisms in astrophysical environments are viscosity, thermal and electrical conduction, and radiation. These predictions are based mainly on the magneto-hydro-dynamic (MHD) equilibrium configuration. Such results on the shock-like structures, accordingly to Lee *et al.* [12], are clearly shaped in such a way that the mechanisms causing the dissipation of magnetic fields (currents) and ions are different in the early phase of shock development. The solar shocks in the form of impulsive blast-wave structures are triggered due mainly to the coronal mass ejections (CMEs), flares and high-energetic disturbances in the solar corona [6-11]. So far is well-known, theoretical investigations [1-7] of such nonlinear waves existing in the Sun, star and their atmospheres which are activated by such mechanisms have boldly been carried out by many researchers. Nevertheless, the combined effects of space charge, plasma-boundary wall interaction and sheath formation mechanism have hardly been addressed in such model stability analyses of the Sun and its atmosphere on the astrophysical (self-gravitational) scales of space and time reported so far in the literature.

Again, from technical point, after the launch of the Solar and Heliospheric Observatory (SOHO) and Transition Region and Coronal Explorer (TRACE) spacecrafts, the direct observations of wave activity in the solar atmosphere are well understood [8-10]. Spacecraft probes (Cluster Mission), experiments, and Earth orbiting satellites like Hinode have also detected many wide-scale nonlinear mode features [8-12]. These include non-propagating pressure-balance structures, collisionless shocks, turbulence-driven instability, soliton, etc. Voyager and Hinode/SOT observations are some more examples on such experimental nonlinear helioseismic investigations. These have particularly been applied to probe plasma kinetic effects, physical properties, and internal structures in the form of collective nonlinear wave activities in some realistic parameter regimes experimentally inaccessible to laboratories due to the complex nature of the dynamics of the Sun, like stars and outflowing wind particles [11-14]. The waves get re-organized and produce charge separation, thereby developing a new variety of waves used in the helioseismic diagnosis of the Sun, its internal structure, and its atmosphere [15-17]. These observations have boosted new research interest in the theory of the helioseismic waves and oscillations in the solar atmosphere, and the collective theory of nonlinear waves, flow energy transports, and their saturated self-similar eigenmodes. The basic physical insights behind these actual mode features are yet to be well understood [15-19]. The best-understood astrophysical collisionless shock observed so far is only the Earth's bow shock, which basically results in the solar wind when the wind interacts with the Earth's magnetosphere [1-2, 5]. A simplified theoretical model, however, is yet to be developed for a better understanding of the observed composite shock signatures and associated complex microphysics.

Apart from the acoustic and electromagnetic waves, the heavy energetic flare particles may develop gravitational waves as well with high intensity ($\sim 10^{26}$ *J*) in the self-gravitating Sun and its atmosphere in course of a few minutes [13-15]. The process involved mainly is the energy transfer from acoustic to gravitational wave form via non-relativistic thermal collisions in the heliospheric plasma. These waves are usually nonlinear and so, they may saturate in the form of corresponding nonlinear eigenmode counterpart [18-20]. Even within the Newtonian gravitational framework [20], such waves are likely to exhibit various nonlinear saturation patterns in the form of solitons, shocks, peakons, kinks, etc. Their study is an emerging and challenging area of present-day scientific research because of their crucial role played in the basic understanding and probing of stellar, galactic and other astrophysical like structure formation mechanism in our universe [11-17].

In this report, we propose a simplified theoretical model to investigate the nonlinear self-gravitational eigenmodes supported in an idealized self-gravitating stellar plasma like the Sun and its atmosphere with the inertialess Boltzmann distributed electrons. This applies the plasma-based gravito-electrostatic sheath (GES) theory [21] proposed recently to understand the basic solar plasma dynamics taking the basic foundation of plasma-boundary wall interaction processes into account. According to the GES model analysis, the entire solar plasma system divides into two elementary parts: the Sun, which is the subsonic solar interior plasma (SIP) on the bounded scale; and the supersonic or hypersonic solar wind plasma (SWP) on the unbounded scale [21-22]. The solar surface boundary (SSB), formed due to the gravito-electrostatic interplay, couples the SIP with the SWP through plasma-boundary wall interaction processes. The GES model with the inertialess electrons is known to support the existence of electrostatic shock-like eigenmodes dictated by the Korteweg-de Vries-Burger (KdV-B) equation [23]. In presence of the active inertial role of the thermal electrons, the eigenmodes evolve as nonmonotonous shock-like structures governed by the extended Burger (*e*-Burger) equation [24]. Besides, the corresponding self-gravitational fluctuations with the electron inertia included exist as monotonous shock-like eigenmodes described by the driven Korteweg-de Vries-Burger (*d*-KdVB) equation [25]. Nevertheless, the self-gravitational eigenmodes with the inertialess electrons are still unknown. Accordingly, the main motivation behind this current investigation is to examine theoretically whether the nonlinear nature [20] of self-gravitational waves is sustained in such situations in presence of the inertialess electrons. Next, the key stimulus is developed to investigate their characteristics and applications of astrophysical importance. We apply the Jeans assumption [26-27] of self-gravitating homogeneous uniform medium adopted for fiducially analytical simplification. This allows us to neglect to neglect the zero-order self-gravitational field [27-28] so that the equilibrium could be treated initially as “homogeneous”.

Apart from the “introduction” part already described in section 1 above, this paper is structurally organized in a standard format as follows. Section 2, as usual, contains physical model of the plasma system under investigation. Section 3 contains basic normalized set of the solar structure equations. Section 4 contains the systematic derivation of the extended Korteweg-de Vries Burger (*e*-KdVB) equation. Section 5 contains the obtained results and possible discussions. Lastly and most importantly, section 6 depicts the main conclusions of scientific interest and astrophysical applicability along with tentative future directions.

2 Physical model

We adopt a simplified solar plasma fluid model to study its self-gravitational nonlinear eigenmode characteristics in a global hydrodynamic equilibrium in presence of the zero-inertia electrons. In the case of stellar or solar plasma, there is no solid boundary wall located at some specified radial position as such, but the self-gravity itself acts as a gravitational potential wall having variable strength in radial direction with the maximum strength at the SSB [21-23]. So, self-gravitationally bounded quasi-neutral field-free plasma by a spherically symmetric surface boundary of non-rigid nature is considered. A bulk non-isothermal flow amid global quasi-neutrality is assumed to pre-exist. For minimalism, we consider spherical symmetry of the self-gravitationally confined SIP mass distribution. It enables us to reduce the three-dimensional (3-D) problem (spherical) for describing the GES into a simplified one-dimensional (1-D) planar problem (radial) with no loss of any generality. The model is developed within the framework of the Jeans homogenization assumption for self-gravitating medium [24-25]. This provides a formal justification for discarding the unperturbed (zero-order) gravitational field, and thereby allows us to regard the equilibrium initially as a homogeneous one (locally). This physically means that self-gravitational potential is sourced only by density fluctuations (and not by unperturbed equilibrium density) of the infinite uniform homogeneous background medium over its equilibrium structure [26-27].

This is to further elucidate that our plasma-based theory of the GES stability is quite simplified in the sense that it does not include any complicacy like the magnetic forces, nonlinear thermal forces, spatio-temporal inhomogeneities of the GES equilibrium and characteristic variables, convective circulation dynamics, and the role of interplanetary medium, or any other difficulties like collisional, viscous processes, and so forth. Besides, the micro-kinetic picture of wave-particle interaction and superdiffusive transport phenomena [29] are also ignored. Because of the non-zero value of the electron-to-ion mass ratio $\left(m_e/m_i \sim 10^{-3}\right)$, a finite difference exists between the electron and ion temperatures in the considered model. However, many authors working on the magnetohydrodynamic (MHD) analyses use isothermal fluid treatment for the solar atmosphere [1-7]. They consider that there is practically no difference in the temperature of the two species in such an atmosphere.

We additionally assume that the entire quasi-neutral solar plasma system consists of a single component of Hydrogen ions as the inertial species and electrons as the thermal species only. The electrons are supposed to obey the Maxwellian population density distribution with gravitational potential term ignored due to their zero-mass approximation. The ions follow

the full inertial dynamics in one dimension of radial degree of freedom. The full inertial response of the ionic dynamical evolution is governed by fluid equations of quasi-hydrostatic equilibrium. This includes the ion fluid momentum equation as well as the ion continuity equation. The first describes the change in ion momentum under the action of the heliocentric gravito-electrostatic field due to self-gravitational potential gradient and forces induced by thermal gas pressure gradient. The latter is considered as a gas dynamic analog of the solar plasma self-similarly flowing through a spherical chamber of radially varying cross-sectional area with macroscopic bulk uniformity in accordance with the basic rule of idealistic fluid flux conservation. This is worth-mentioning that all the model equations being considered here is in the nonrelativistic classical limit of the Newtonian gravity without involving any contribution from the general theory of relativity meant for the Minkowski space. This model setup sustains nonlinearity due to fluidity, dispersion due to self-gravity within geometrical curvature and dissipation due to collective collisional dynamics of intrinsic solar origin. The strength of the electric forces developed due to space charge polarization effects (local charge imbalance) are taken to be too weak to excite higher order contributions of the various nonlinear terms on the Jeans scale, thereby validating our underlying assumption of weak nonlinearity.

3 Basic normalized set of structure equations

Applying the conventional normalization procedure with all the standard astrophysical parameters, the basic normalized autonomous set of nonlinear differential equations with all the usual notations [21] constituting a closed hydrodynamical structure of the solar plasma has already been developed in time-stationary form. With the electronic dynamics described by the Boltzmann population density distribution function $N_e = e^{\theta}$ only, the same set of the basic solar structure equations consisting of the ion momentum equation, continuity equation, the closing electrostatic Poisson equation and self-gravitational Poisson equation on the astrophysical scale of space and time in non-autonomous form are enlisted, respectively, as follows,

$$\frac{\partial M}{\partial \tau} + M\frac{\partial M}{\partial \xi} = -\alpha\frac{\partial \theta}{\partial \xi} - \frac{\partial \eta}{\partial \xi}, \tag{1}$$

$$\frac{\partial \theta}{\partial \tau} + \frac{2}{\xi}M + \frac{\partial M}{\partial \xi} + M\frac{\partial \theta}{\partial \xi} = 0, \tag{2}$$

$$\left(\frac{\lambda_{De}}{\lambda_J}\right)^2\left(\frac{\partial^2 \theta}{\partial \xi^2} + \frac{2}{\xi}\frac{\partial \theta}{\partial \xi}\right) = e^{\theta} - N_i \text{ and} \tag{3}$$

$$\frac{2}{\xi}\frac{\partial \eta}{\partial \xi}+\frac{\partial^2 \eta}{\partial \xi^2}=N_i-N_{i0}, \qquad (4)$$

where, the normalized equilibrium density N_{i0} (=1) models the Jeans swindle of the equilibrium unipolar gravitational force field, which is a kind of local approximation for the equilibrium self-gravitating mass distribution [26-27]. This provides a formal justification for discarding the unperturbed (zero-order) gravitational field, and thereby allows us to regard the equilibrium initially as a homogeneous one (locally). This physically means that self-gravitational potential is sourced only by density fluctuations (and not by unperturbed equilibrium density) of the infinite uniform homogeneous background medium over its equilibrium structure [26-27]. The Jeans assumption (ad hoc) for the self-gravitating uniform homogeneous medium may not be the most suitable one, but it allows us to treat the self-gravitating inhomogeneous plasma analytically in a simplified way [27]. The results based on this homogenization assumption in most cases have been found to be not far from the large-scale realistic picture of astrophysical dynamics [27-28].

The significance of various notations is as follows. Here , $\alpha=(1+\in_T)$ and $\in_T$ is the ratio of ion-to-electron temperatures (each in energy unit of eV). The parameters $M(\xi)$, $\theta(\xi)$ and $\eta(\xi)$ represent the normalized ion flow Mach number, electrostatic potential and solar self-gravitational potential, respectively. They are respectively normalized by the plasma sound phase speed (c_s), electron thermal potential (T_e/e) and plasma phase speed squared (c_s^2). The independent variables like time (τ) and position (ξ) are normalized with the Jeans time (ω_J^{-1}) and Jeans length (λ_J) scales, respectively. Moreover, $N_i=N_i$ and $N_e=e^{\theta}$ are respectively the ion and electron population densities normalized by the equilibrium bulk plasma population density (n_o). Rest of all other notations, terms and model justifications are same as in our earlier publications [21-25]. The coupled set of above equations (1)-(4) will be applied for investigating the self-gravitating solar fluctuation dynamics of our present concern.

The normalization in most of the practical situations of astrophysical significance is carried out by the equilibrium values (on an average) of the relevant physical parameters, which are usually treated as constants. The assumption of uniform behavior of the equilibrium plasma parameters is an idealized one and valid only locally in the radial direction [26]. We admit that our normalization parameter values may be taken to be constant at a particular spatio-temporal point only in the Sun. Since, self-gravitating

plasmas are inhomogeneous in nature, these parameters keep on changing globally in radial direction. But, to see the fluctuation dynamics in an idealized situation as in the present situation, we pre-summed them as constants. Our approach is justifiable on the basis of the Jeans assumption of homogeneous medium in mathematical simplification for nonlinear local node analyses [26-28].

4 Derivation of extended KdV-Burger equation

We apply a standard multiple scaling technique [3-5,28,30] over equations (1)-(4) to see the self-gravitational fluctuations with the Boltzmannian electrons on the Jeans scale. Procedurally, the independent relevant variables with all usual notations are stretched into a new space coordinatized by the stretching transformations $X = \in^{1/2} (\xi - \mu\tau)$ and $T = \in^{3/2} \tau$. In the new space, the differential operators get transformed as $\partial/\partial\xi = \in^{1/2} \partial/\partial X$, $\partial^2/\partial\xi^2 = \in\partial^2/\partial X^2$ and $\xi = X \in^{-1/2} + \mu T \in^{-3/2}$, where μ is the phase speed of the fluctuations and $\in$ is a minor parameter characterizing the dimensionless amplitude of the lowest-order fluctuations [3-5]. The solar physical variables (M, η, θ, N_i) are now perturbatively expanded around the respective GES equilibrium values $(M_o, \eta_o, \theta_o, N_o)$ in weak nonlinearity approximation as follows

$$\begin{pmatrix} N_i \\ M \\ \theta \\ \eta \end{pmatrix} = \begin{pmatrix} N_{io} \\ M_o \\ \theta_o \\ \eta_o \end{pmatrix} + \in \begin{pmatrix} N_{i1} \\ M_1 \\ \theta_1 \\ \eta_1 \end{pmatrix} + \in^2 \begin{pmatrix} N_{i2} \\ M_2 \\ \theta_2 \\ \eta_2 \end{pmatrix} + \ldots\ldots\ldots\ldots \quad (5)$$

Our equilibrium is initially assumed as a homogeneous one. So, there is no fluctuation considered in the equilibrium parameter values with N_{i0}=1, and all other equal to zero. We now substitute equation (5) in equations (1)-(4). Equating the like terms on various powers of $\in$ from both sides of equation (1), one gets

$$\in^{3/2}: M_o \frac{\partial M_1}{\partial X} - \mu \frac{\partial M_1}{\partial X} = -\alpha \frac{\partial \theta_1}{\partial X} - \frac{\partial \eta_1}{\partial X}, \quad (6)$$

$$\in^{5/2}: \frac{\partial M_1}{\partial T} - \mu \frac{\partial M_2}{\partial X} + M_o \frac{\partial M_2}{\partial X} + M_1 \frac{\partial M_1}{\partial X} = -\alpha \frac{\partial \theta_2}{\partial X} - \frac{\partial \eta_1}{\partial X}, \quad (7)$$

$$\in^{7/2}: \frac{\partial M_2}{\partial T} + M_1 \frac{\partial M_2}{\partial X} + M_2 \frac{\partial M_1}{\partial X} = 0, \quad (8)$$

$$\in^{9/2}: M_2 \frac{\partial M_2}{\partial X} = 0, \text{ and so on.} \quad (9)$$

Similarly, equating the terms in various powers of $\in$ from both sides of equation (2), one gets

$$\in^{0}: \frac{2}{X}\left(M_o - \frac{\mu T M_1}{X}\right) = 0, \tag{10}$$

$$\in^{1}: \frac{2}{X}\left(M_1 - \frac{\mu T M_2}{X}\right) = 0, \tag{11}$$

$$\in^{3/2}: M_o \frac{\partial \theta_1}{\partial X} - \mu \frac{\partial \theta_1}{\partial X} + \frac{\partial M_1}{\partial X} = 0, \tag{12}$$

$$\in^{5/2}: \frac{\partial \theta_1}{\partial T} - \mu \frac{\partial \theta_2}{\partial X} + M_o \frac{\partial \theta_2}{\partial X} + M_1 \frac{\partial \theta_1}{\partial X} + \frac{\partial M_2}{\partial X} = 0, \tag{13}$$

$$\in^{7/2}: \frac{\partial \theta_2}{\partial T} + M_1 \frac{\partial \theta_2}{\partial X} + M_2 \frac{\partial \theta_1}{\partial X} = 0, \tag{14}$$

$$\in^{9/2}: M_2 \frac{\partial \theta_2}{\partial X} = 0, \text{ and so on.} \tag{15}$$

The same order-by-order analysis in various powers of $\in$ from equation (3) yields

$$\in^{1}: \left(\frac{\lambda_{De}}{\lambda_J}\right)^2 \left(-\frac{2}{X^2}\mu T \frac{\partial \theta_1}{\partial X}\right) = \theta_1 - N_{i1}, \tag{16}$$

$$\in^{2}: \left(\frac{\lambda_{De}}{\lambda_J}\right)^2 \left(\frac{\partial^2 \theta_1}{\partial X^2} + \frac{2}{X}\frac{\partial \theta_1}{\partial X} - \frac{2}{X^2}\mu T \frac{\partial \theta_2}{\partial X}\right) = \theta_2 - N_{i2}, \tag{17}$$

$$\in^{3}: \left(\frac{\lambda_{De}}{\lambda_J}\right)^2 \left(\frac{\partial^2 \theta_2}{\partial X^2} + \frac{2}{X}\frac{\partial \theta_2}{\partial X}\right) = 0, \text{ and so forth.} \tag{18}$$

The order-by-order analysis in $\in$-powers from equation (4) similarly yields

$$\in^{1}: -\frac{2\mu T}{X^2}\frac{\partial \eta_1}{\partial X} = N_{i1}, \tag{19}$$

$$\in^{2}: \frac{2}{X}\frac{\partial \eta_1}{\partial X} - \frac{2\mu T}{X^2}\frac{\partial \eta_2}{\partial X} + \frac{\partial^2 \eta_1}{\partial X^2} = N_{i2}, \tag{20}$$

$$\in^{3}: \frac{2}{X}\frac{\partial \eta_2}{\partial X} + \frac{\partial^2 \eta_2}{\partial X^2} = 0, \text{ and so on.} \tag{21}$$

After simplifying equation (20), by systematically eliminating the second-order perturbed quantities using various expressions enlisted in equations (6)-(21) in accordance with the conventional procedure [3-5,28,30], we get the following extended Korteweg-de Vries Burger (*e*-KdVB) equation relating the self-gravitation fluctuations (in terms of η_1) on the Jeans scale,

$$\frac{\partial \eta_1}{\partial T} + \gamma_1 \eta_1 \frac{\partial \eta_1}{\partial X} + \gamma_2 \frac{\partial^3 \eta_1}{\partial X^3} + \gamma_3 \frac{\partial^2 \eta_1}{\partial X^2} + \gamma_4 \frac{\partial \eta_1}{\partial X} + \gamma_5 \eta_1 = 0, \quad (22)$$

where,

$$\gamma_1 = Z = \left[(M_o - \mu)/\alpha - (M_o - \mu)^2 \right], \quad (23)$$

$$\gamma_2 = \frac{\alpha + \left(\frac{\lambda_{De}}{\lambda_J} \right)^2 \{1 - (M_o - \mu)Z\}}{Z}, \quad (24)$$

$$\gamma_3 = \frac{2\alpha + \left(\frac{\lambda_{De}}{\lambda_J} \right)^2 2\{1 - (M_o - \mu)Z\}}{XZ}, \quad (25)$$

$$\gamma_4 = \frac{X^3 (M_o - \mu)Z - \left(\frac{\lambda_{De}}{\lambda_J} \right)^2 2\mu T \{1 - (M_o - \mu)Z\} - 2\mu T \alpha}{X^2 Z \mu T}, \text{ and} \quad (26)$$

$$\gamma_5 = \frac{(M_o - \mu)}{\mu T}. \quad (27)$$

We are interested in the time-stationary structures of the self-gravitational fluctuations and their evolutions. So, equation (22) is transformed to an ordinary differential equation (ODE) with the conventional Galilean type of transformation $\xi = X - VT$ with normalized velocity $V = 1$ without any loss of generality. The operator equivalence $\partial/\partial X = \partial/\partial \xi$ and $\partial/\partial T = -\partial/\partial \xi$ hold good even in new co-moving frame of reference. Thus, the following steady-state form of equation (22) in the new slow space coordinate (ξ) is obtained,

$$\frac{\partial \eta_1}{\partial \xi} - \gamma_1 \eta_1 \frac{\partial \eta_1}{\partial \xi} - \gamma_2 \frac{\partial^3 \eta_1}{\partial \xi^3} - \gamma_3 \frac{\partial^2 \eta_1}{\partial \xi^2} - \gamma_4 \frac{\partial \eta_1}{\partial \xi} - \gamma_5 \eta_1 = 0. \quad (28)$$

Equation (28) represents the steady-state form of the *e*-KdVB equation governing the nonlinear fluctuation evolution. It can further be simplified as follows,

$$\frac{\partial \eta_1}{\partial \xi} + \frac{\gamma_1}{(\gamma_4 - 1)} \eta_1 \frac{\partial \eta_1}{\partial \xi} + \frac{\gamma_2}{(\gamma_4 - 1)} \frac{\partial^3 \eta_1}{\partial \xi^3} + \frac{\gamma_3}{(\gamma_4 - 1)} \frac{\partial^2 \eta_1}{\partial \xi^2} = -S_i(\xi), \text{ where} \quad (29)$$

$$S_i(\xi) = \frac{\gamma_5}{(\gamma_4 - 1)} \eta_1. \quad (30)$$

Here, $S_i(\xi)$ represents the transformed linear sink (damping source) arising due mainly to solar internal dissipative processes through collective

dynamics through self-gravity. Equation (29) evidently shows the possibilities for the existence of the nonlinear eigenmode excitations in the form of shock-like structures (due to energy dissipation) in addition to soliton-like structures (due to energy dispersion). The first class of structures realistically arises when the effect of dissipation is significant in comparison with the joint effect of the nonlinearity and dispersion, whereas, for the second class, the effect of dissipation is insignificant in comparison with that produced jointly by the nonlinearity and dispersion [3-5].

5 Results and discussions

Our study shows that the nonlinear self-gravitational stability of the idealized solar plasma within the GES model framework is governed by a unique *e*-KdVB equation (29). Clearly, it analytically supports possibilities for the existence of two distinct classes of nonlinear eigenmode spectra as soliton-like (for less dissipation) and shock-like (for more dissipation) structures. To get the exact picture, equation (29) is numerically solved (by the fourth-order Runge-Kutta method) as an initial value problem under judiciously chosen disparate conditions [3-8, 21-23]. The details of the numerical fluctuation patterns are displayed in Figures (1)-(8).

Figure 1 shows the spatial profile of the lowest-order perturbed self-gravitational (a) potential, (b) potential gradient, and (c) phase space portraits on the bounded scale. Various lines correspond to Case (1): $\in_T = 0.1$ (blue line), Case (2): $\in_T = 0.2$ (red line), Case (3): $\in_T = 0.3$ (green line), and Case (4): $\in_T = 0.4$ (black line), respectively. Different initial values used are $\eta_i = 0$, $\left(\eta_\xi\right)_i = 10^{-3}$, and $\left(\eta_{\xi\xi}\right)_i = 10^{-3}$. The other input parameters kept fixed are $M_o = 10^{-8}$, $\mu = 0.1$, $\in = 10^{-2}$, $T = 35.00$, and $(\lambda_{De}/\lambda_J) = 10^{-20}$. It demonstrates the existence of oscillatory soliton-like eigenmodes due to the periodic interplay between nonlinear (due to fluidity) and dispersive (due to self-gravity) effects. Evidently, there are oscillations trailing behind the propagating solitons due to coupling with the background small-scale fluctuations. The oscillation amplitudes undergo damping due to the presence of the linear sink term in equation (29). The oscillation amplitude is found to be more before the SSB is reached on the SIP scale, beyond which the fluctuation almost comes to the zero-level. The extended version of Figure 1 on the SWP scale is depicted in Figure 2. The trajectories of the phase portrait (Figures 1(c)-2(c)) reveal that the heliocentre is the most stable fixed point in the defined phase space (by potential and its gradient). The stability increases as we move away from the heliocentre asymptotically outward relative to the center. The self-gravitational instability of the SIP may be due to the micro-inhomogeneities (due to deviation from mass-

neutrality) in the material distribution of the heavier ions under the influence of the ambipolar diffusion processes leading to some space-charge polarization effect. In addition, as $\in_T$ increases, the amplitude of self-gravitational potential increases on both the bounded and unbounded scales under the GES force balancing.

Figure 3 portrays the same as Figure (1). But, various lines correspond to Case (1): $T = 35$ (blue line), Case (2): $T = 50$ (red line), Case (3): $T = 65$ (green line), and Case (4): $T = 80$ (black line), respectively. Different initial values used are $\eta_i = 0$, $(\eta_\xi)_i = 10^{-3}$, and $(\eta_{\xi\xi})_i = 10^{-3}$. The other input parameters kept constant are $M_o = 10^{-8}$, $\mu = 1.17$, $\in_T = 0.4$, and $(\lambda_{De}/\lambda_J) = 10^{-20}$. It shows the excitations of oscillatory shock-like structures due to the significant effect of internal dissipation in comparison with the joint effect of the nonlinearity and dispersion. The gradual damping of oscillation amplitude is due to the presence of the sink. The SWP-extension of Figure 3 is displayed in Figure 4. It is seen that the global amplitude of the perturbed self-gravitational potential and its gradient are highly damped out due to the combined contribution of the solar external gravity through the linear sink.

Figure 5 gives the same as Figure (1). But, now various lines correspond to Case (1): $\in_T = 0.37$ (blue line), Case (2): $\in_T = 0.38$ (red line), Case (3): $\in_T = 0.39$ (green line), and Case (4): $\in_T = 0.4$ (black line), respectively. Different initial values used are $\eta_i = 0$, $(\eta_\xi)_i = 10^{-3}$, and $(\eta_{\xi\xi})_i = 10^{-3}$. The other input parameters kept constant are $M_o = 10^{-8}$, $\mu = 1.16$, $T = 65$, and $(\lambda_{De}/\lambda_J) = 10^{-20}$. Figure 6 describes the unbounded extension of Figure 5. It reveals that with slight increase in $\in_T$, the global amplitude of the oscillatory local shock-like eigenmodes also increases, which is in accordance with earlier Figure 1(a).

Figure 7 gives the same as Figure (1). Various lines correspond to Case (1): $\mu = 1.15$ (blue line), Case (2): $\mu = 1.16$ (red line), Case (3): $\mu = 1.17$ (green line), and Case (4): $\mu = 1.18$ (black line), respectively. Different initial values used are $\eta_i = 0$, $(\eta_\xi)_i = 10^{-3}$, and $(\eta_{\xi\xi})_i = 10^{-3}$. The other input parameters kept constant are $M_o = 10^{-8}$, $\in_T = 0.4$, $T = 65$, and $(\lambda_{De}/\lambda_J) = 10^{-20}$. Figure 7(a) also shows damped oscillatory shock-like eigenmode structures. It is clear that with increase in reference frame velocity (μ), the global amplitude of perturbed potential decreases, and also, the stability of the SIP is highly disturbed as shown by the phase portraits

(Figure 7(c)). Figure 8 displays the same as Figure (7), but on the unbounded scale.

In all the above numerical profiles (Figures 1-8), it is clear that the average amplitude (global) of the perturbed self gravitational potential is $\approx 10^{-3}$. Thus, for $\in \approx 10^{-2}$ and $c_s^2 \approx 9.00 \times 10^{10}$ $m^2 s^{-2}$ for $T_e \approx 10^7$ K [21-25], the physical value of the fluctuation is $\eta_{phy}(\xi) = \in \eta_1(\xi) \approx 10^{-5} \sim 10^6$ J kg^{-1}, which is very less as compared with that of the equilibrium self-gravitational potential $\approx 1.26 \times 10^{11}$ J m^{-1} on the SIP, and so forth. On an averaging process, the obtained results on the soliton- and shock-like features are in qualitative agreement with various other model predictions [1-7], multispace satellite (like Hinode, Cluster, TRACE, etc) data [8-11] and experimental observations [12-14]. Although simplified and idealized, the analyses may possibly have extensive applications in probing the deep interior of the Sun, like stellar structure, and their atmospheres [15-17].

We must admit that this idealized model description presents a simple attempt to apply a previously developed GES model for the explanation of various phenomena observed on the Sun and its atmosphere in the current investigation of fluctuations. However, the theory of collisionless plasma without magnetic field is not realistic for describing the Sun [1-6, 11-15]. Except the solar corona and solar wind, the mean-free path of the electrons and ions is much smaller than the scales of the observed phenomena, and thus, a theory of collisionless plasma is not physically applicable for the most accurate form of expected results [5-6]. In addition, solar observations provide many direct evidences (through various spectro-polarimetric measurements) of strong magnetic fields, and show that for most phenomena like CME, flares, etc. the plasma parameter beta is much less than unity, particularly, in the corona and wind [5-6, 12-14]. Thus, magnetic fields need to be taken into account for a better and more accurate form of picture of the solar dynamic phenomena. Therefore, the presented theory gives only the idealized form of the basic nonlinear properties of the solar plasma in a simplified way along with their relevant graphical characterizations in elaboration.

We understand that our investigation demonstrates the nonlinear eigenmode spectral patterns in terms of the weakly perturbed self-gravitational potential based on normal mode analyses (local) in presence of scrawny nonlinearity and dispersion in the complicated stratified Sun. But, the self-gravitating plasmas, like the Sun, are known to be inhomogeneous in nature, and thus, adopting constant normalization parameter values of the solar variables throughout the entire Sun is not so physically justifiable [26]. Indeed, a spatially homogeneous self-gravitating plasma system cannot be in static equilibrium, since there is no pressure gradient to balance the

gravitational force. Therefore, the Jeans assumption of self-gravitating homogeneous medium to get rid of the inhomogeneous complication [26-27] in mathematical simplification is invoked. The Jeans assumption (ad hoc) might not be the most suitable, but it allows us to treat the self-gravitating plasma dynamics analytically in a simplified way. The obtained results on such fluctuation dynamics based on this homogenization assumption in most cases are not far from reality, both in absence [26-29] and in presence of superdiffusion [30].

6 Conclusion

In this paper, an idealized model is theoretically proposed to study the nonlinear self-gravitational fluctuation dynamics in the complicated solar plasma system with the help of the plasma-based GES formalism in a field-free hydrodynamic equilibrium configuration on the Jeans scale. The self-gravitational fluctuations are collectively governed by a unique form of the *e*-KdVB equation having a linear sink on the lowest-order self-gravitational potential fluctuation contributed by the heavier ionic fluid in presence of the Boltzmann electrons. This equation is a methodological and strategic outcome of the multiscale analysis over the simplified solar structure equations basing on the Jeans assumption of homogeneous medium for generalization.

Being of highly nonlinear type, the *e*-KdVB equation is integrated numerically only as an initial value problem (Runge-Kutta fourth-order method) to see the exact parametric details of the fluctuation spectra in detail. Our numerical shape-analysis with multi-parameter variation depicts the co-existence of two distinct classes of new nonlinear eigenmode excitations. They evolve as *oscillatory soliton-like* and *oscillatory shock-like* patterns in judicious plasma conditions. Their oscillations, arising due to resonant and non-resonant coupling phenomena, get gradually damped out due to the active sink. This specific example of our self-gravitational stability analysis on the GES model shows resonant coupling (in phase and amplitude coordination) and non-resonant coupling (out of phase and amplitude coordination) of the internal spectral components of the usual KdVB eigenmodes (solitons and shocks), and the background self-gravitational microscale fluctuations. The amplitude of the oscillations trailing behind the KdVB eigenmodes, known as self-gravitational precursor or self-gravitational wind, is asymptotically damped out due to the presence of the self-consistent linear sink. Their characteristic features on an average are in qualitative agreement with the multispace satellite observations and experimental findings. A detailed geometrical interpretation (phase trajectories) to see the global behavior of the eigenmodes is also presented.

Although simplified and idealized in approach, we strongly believe that this work presents a new theoretical study of a special branch of nonlinear waves in the self-gravitating solar plasma governed by the *e*-KdVB dynamics based on a technique centered around a standard multiscale analysis with weak nonlinearity (~3^{rd} order) along with an elaborative multi-parameter variation numerical characterization. The unique oscillatory nature of the self-gravitational solitons and shocks explored are due to the presence of the inertialess electrons, in contrast with our earlier studies [23-25]. Thus, unlike the previous works carried out by others [3-8] and by us [23-25], a new conclusive remark is derived that our model supports self-gravitational stationary solitary (shock) waves having tails (fronts) composed of a sequence of slightly overlapping solitons with smoothly varying characteristic parameters. Their formation mechanisms are the consequences of self-gravitational dissipative or non-conservative dynamics (clear from open global phase trajectories). The adopted methodologies and techniques, after proper refinements [1-6, 30] with external electromagnetic fields, superdiffusive transport phenomena and collisional counterparts in the physical bedrock, may be extended to study the fluctuations in gravito-acoustically turbulent plasmas [30] in practical situations. In addition, the results may be applied as a helioseismic tool to probe the deep-interior structure of the Sun, like star and their mysterious atmospheres in a simplified manner. To summarize and conclude in brief, the main points which may be drawn from our idealized theoretical analysis on the complex stratified solar plasmas are highlighted as follows.

(1) The GES-induced self-gravitational fluctuations in the idealized solar plasma system are collectively governed by a unique form of the *e*-KdVB equation involving a linear sink.

(2) The dynamical evolution of the fluctuations arises due to the massive (inertial) ions only.

(3) The solar plasma model supports new *oscillatory soliton-like* and *oscillatory shock-like* eigenmode excitations amid periodic gravito-electrostatic coupling processes.

(4) The global (average) amplitude of the fluctuations is maximum in the SIP due to the high population density of the inertial ions.

(5) The amplitude of the perturbed self-gravitational potential increases with the electron-to-ion temperature ratio, and vice versa.

(6) With increase of reference frame velocity, the eigenmode amplitude decreases and vice versa.

(7) Maximum fluctuation strengths are pronounced on the SIP; and on the SWP scale, all the profiles depict almost quasi-linear behaviors.

(8) With increase in observation time scale, there is almost no change in the global amplitude of the self-gravitational fluctuations in the entire SIP.

But in the SWP, the difference in amplitude is noticeable as direct functional dependence on the interfacial scale transition.

(9) The damping nature of the eigenmode amplitude is due to the presence of self-consistent sink term in the governing *e*-KdVB equation.

(10) The crests and troughs in the local amplitude of oscillations are due to resonant (in phase) and non-resonant (out of phase) interaction of the self-gravitational winds (spectral components of wave-packet model) and background microscale fluctuations.

(11) The different phase portraits depicting the global geometry of the involved dynamics of the fluctuations show that the SIP is more unstable, and stability increases outward asymptotically to the unbounded scale relative to the center of the entire solar plasma mass distribution.

(12) The nonlinear waves (shock-like) may play an important role in particle acceleration to very high energy (~1-10 MeV) in the SWP, which in turn can mean that (diffusive) shock-acceleration [30] is one of the main mechanisms for particle acceleration, for which our analyses may give some theoretical support in space and astrophysical environments.

(13) And lastly, we hope that the adopted model methodologies may be used as elementary inputs in the asteroseismic and helioseismic wave studies in realistic astrophysical situations. In addition, this contribution may be an initial step likely to have extensive future applications to investigate the nonlinear wave dynamics in heliospheric dusty plasma after proper inclusion of evolutionary model describing the solar dust grains and grain-distributions [31].

References:

R.F. Stein and J. Leibacher, Ann. Rev. Astron. Astrophys. **12**, 407 (1974)
C.F. McKee and D.J. Hollenbach, Ann. Rev. Astron. Astrophys. **18**, 219 (1980)
I. Ballai, Astron. Astrophys. **404**, 701 (2003)
I. Ballai, PADEU **15**, 73 (2005)
V.M. Nakariakov and E. Verwichte, Liv. Rev. Sol. Phys. **2**, 3 (2005) (http: //livingreviews.org/lrsp-2005-3)
M.S. Ruderman, Phi. Trans. R. Soc. A **364**, 485 (2006)
I. Ballai, E. Forgacs and A. Marcu, Astron. Nachr. **328**, 734 (2007)
B. Vršnak and E.W. Cliver, Sol. Phys. **253**, 215 (2008)
T.V. Zaqarashvili, V. Kukhianidze and M.L. Khodachenko, Mon. Not. R. Astron. Soc. **404**, L74 (2010)
L. Ofman and T.J. Wang, Astron. Astrophys. **482**, L9 (2008)
J.-M. Malherbe, T. Roudier, M. Rieutord, T. Berger and Z. Franck, Sol. Phys. **278**, 241 (2012)

E. Lee, G.K. Parks, M. Wilber and N. Lin, Phys. Rev. Letts. **103**, 031101 (2009)
A.M. Veronig, P. Gomory, I.W. Kienreich, N. Muhr, B. Vrsnak, M. Temmer and H.P. Warren, Astrophys. J. Letts. **743**, L10 (2011)
A.M. Veronig, P. Gomory, I.W. Kienreich, N. Muhr, B. Vršnak, M. Temmer and H.P. Warren, Astrophys. J. Letts. **745,** L18 (2012)
F.-L. Deubner and D. Gough, Ann. Rev. Astron. Astrophys. **22**, 593 (1984)
P. Demarque and D.B. Guenther, Proc. Nat. Acad. Sci. **96**, 5356 (1999)
A.G. Kosovichev, Adv. Space Res. **37**, 1455 (2006)
T.M. Rogers and G.A. Glatzmaier, Mon. Not. R. Astron. Soc. **364**, 1135 (2005)
D.M. Siegel and M. Roth, Astrophys. J. **729**, 137 (2011)
C. Yi-Fang, Apeiron **3**, 30 (1996)
C.B. Dwivedi, P.K. Karmakar and S.C. Tripathy, Astrophys. J. **663**, 1340 (2007)
P.K. Karmakar and C.B. Dwivedi, Int. J. Astron. Astrophys. **2011**, 210 (2011)
P.K. Karmakar, Phys. Res. Int. **2011**, 1 (2011)
P. K. Karmakar and B. Bora, J. Sci. **3** 215 (2013)
P. K. Karmakar and B. Bora, Contrib. Plasma Phys., pp. 1-24, 2013 (DOI 10.1002/ctpp.201200132).
V.M. Cadez, Astron. Astrophys. **235**, 242 (1990)
J. Vranjes, Astrophys. Space Sci. **213**, 139 (1994)
F.Verheest and P.K. Shukla, Phys. Scripta **55**, 83 (1997)
P.H. Chavanis, Eur. Phys. J. B **85** 229 (2012)
G. Zimbardo, S. Perri, P. Pommois and P. Veltri, Adv. Space Res. **49**, 1633 (2012)
S. Mahmood and H. Ur-Rehman, Phys. Plasmas **17** 072305 (2010)
H. Krüger and E. Grün, Space Sci. Rev. **143** 347 (2009)

Figures

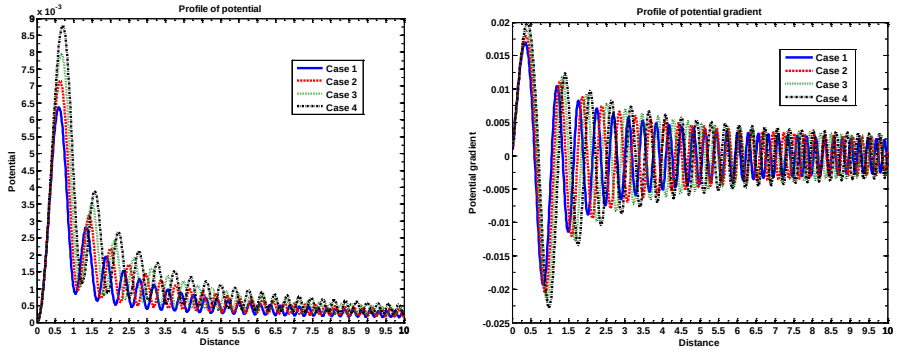

(a) (b)

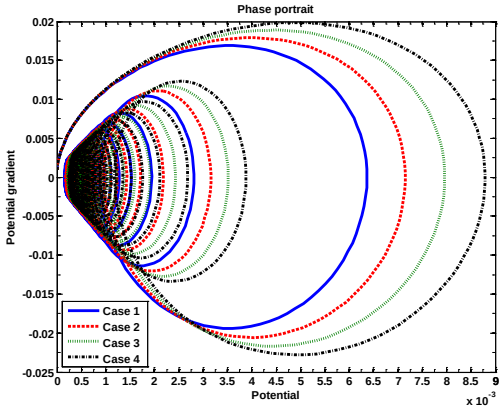

(c)

Fig. 1. Profile of the lowest-order perturbed self-gravitational (a) potential, (b) potential gradient, and (c) phase space portraits on the bounded scale. Various lines correspond to Case (1): $\in_T = 0.1$ (blue line), Case (2): $\in_T = 0.2$ (red line), Case (3): $\in_T = 0.3$ (green line), and Case (4): $\in_T = 0.4$ (black line), respectively. Different initial values used are $\eta_i = 0$, $\left(\eta_\xi\right)_i = 10^{-3}$, and $\left(\eta_{\xi\xi}\right)_i = 10^{-3}$. The other input parameters kept fixed are $M_o = 10^{-8}$, $\mu = 0.1$, $\in = 10^{-2}$, $T = 35.00$, and $\left(\lambda_{De}/\lambda_J\right) = 10^{-20}$.

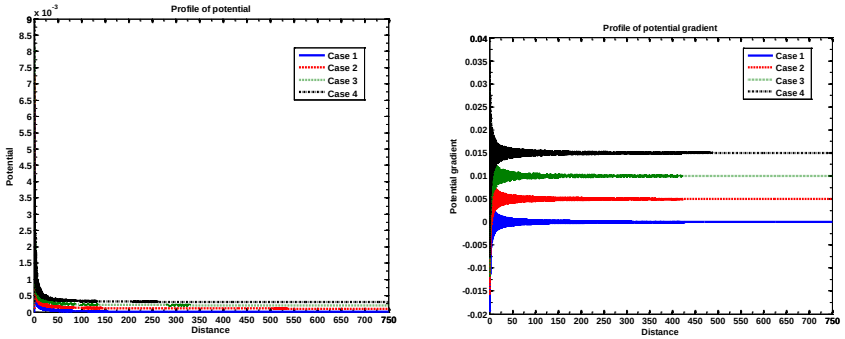

(a) (b)

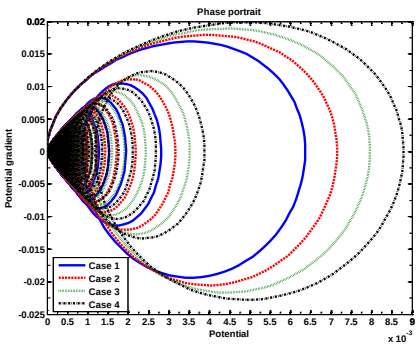

(c)

Fig. 2. Same as Figure (1), but on the unbounded scale.

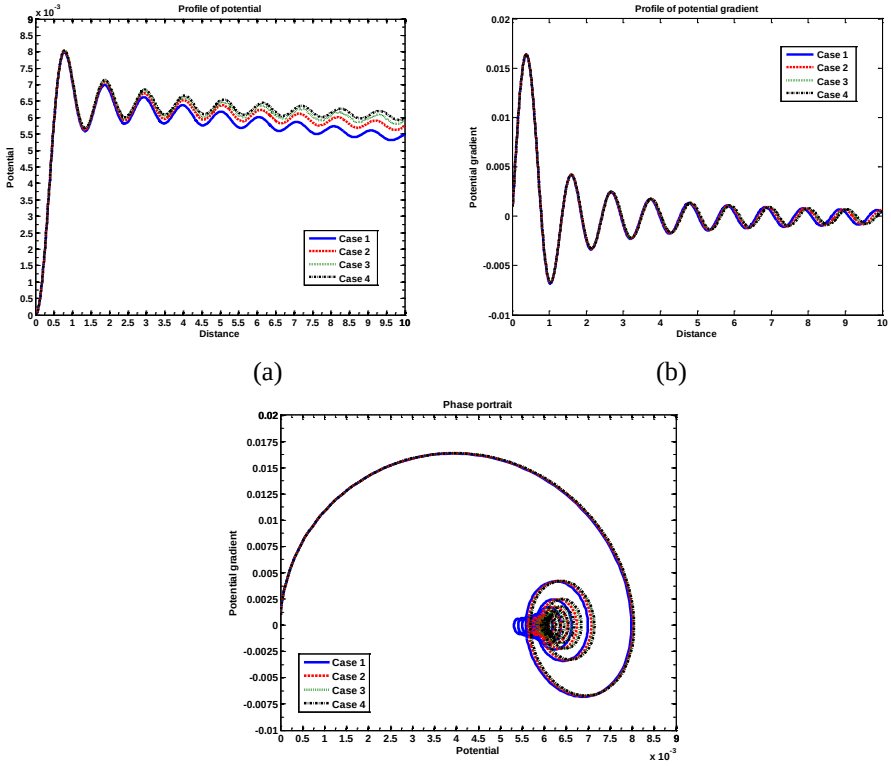

Fig. 3. Same as Figure (1). Various lines correspond to Case (1): $T = 35$ (blue line), Case (2): $T = 50$ (red line), Case (3): $T = 65$ (green line), and Case (4): $T = 80$ (black line), respectively. Different initial values used are $\eta_i = 0$, $\left(\eta_\xi\right)_i = 10^{-3}$, and $\left(\eta_{\xi\xi}\right)_i = 10^{-3}$.

The other input parameters kept constant are $M_o = 10^{-8}$, $\mu = 1.17$, $\in_T = 0.4$, and $\left(\lambda_{De}/\lambda_J\right) = 10^{-20}$.

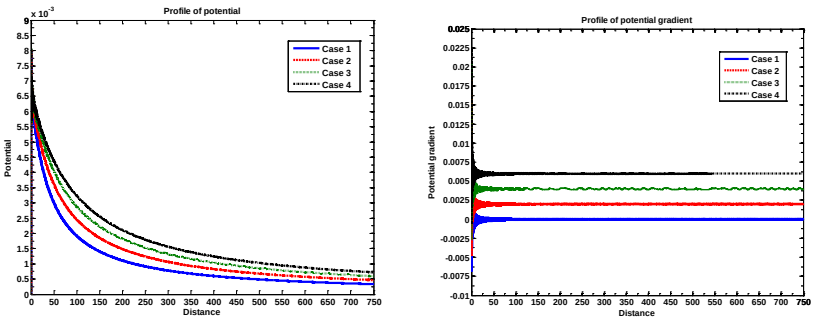

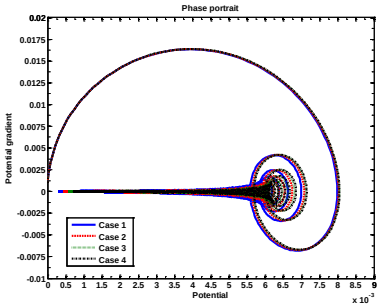

(c)

Fig. 4. Same as Figure (3), but on the unbounded scale.

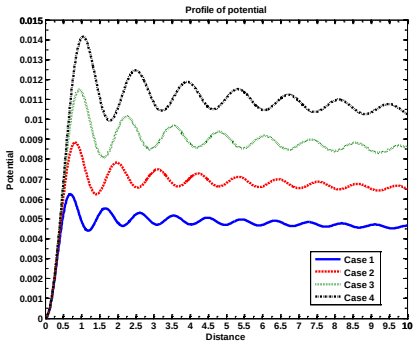

(a)

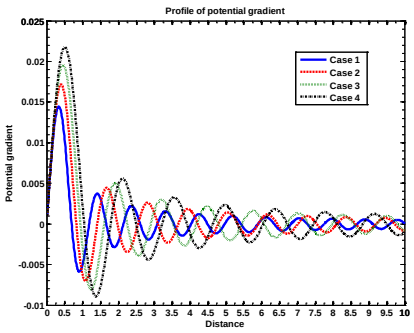

(b)

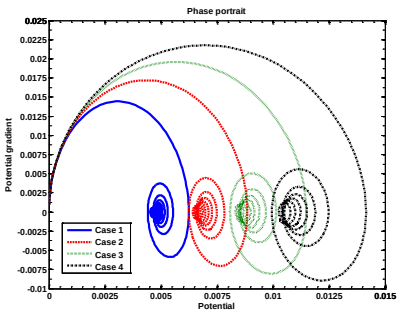

(c)

Fig. 5. Same as Figure (1). Various lines correspond to Case (1): $\in_T = 0.37$ (blue line), Case (2): $\in_T = 0.38$ (red line), Case (3): $\in_T = 0.39$ (green line), and Case (4): $\in_T = 0.4$ (black line), respectively. Different initial values used are $\eta_i = 0$, $\left(\eta_\xi\right)_i = 10^{-3}$, and $\left(\eta_{\xi\xi}\right)_i = 10^{-3}$. The other input parameters kept constant are $M_o = 10^{-8}$, $\mu = 1.16$, $T = 65$, and $\left(\lambda_{De}/\lambda_J\right) = 10^{-20}$.

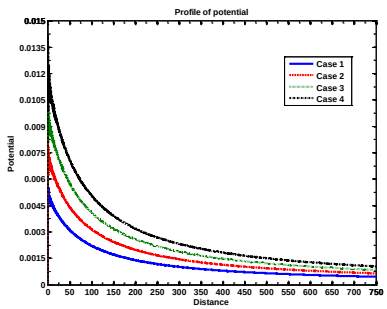

(a)

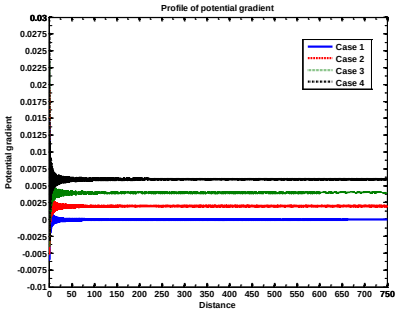

(b)

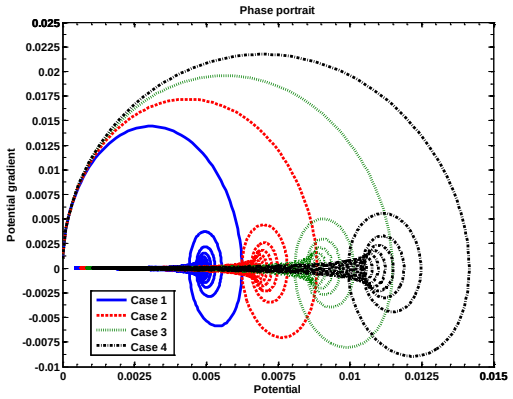

(c)

Fig. 6. Same as Figure (5), but on the unbounded scale.

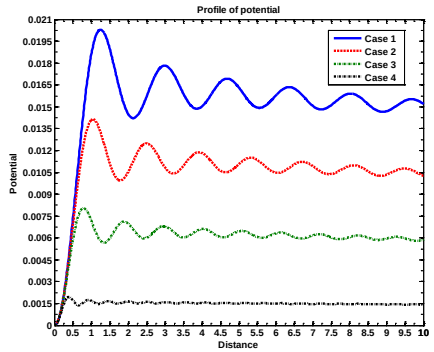

(a)

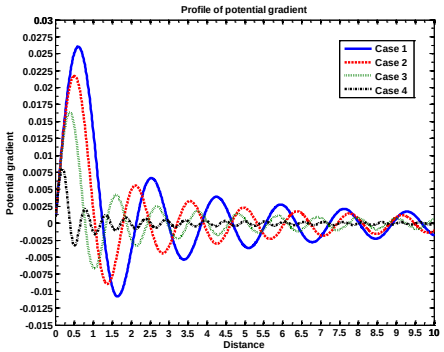

(b)

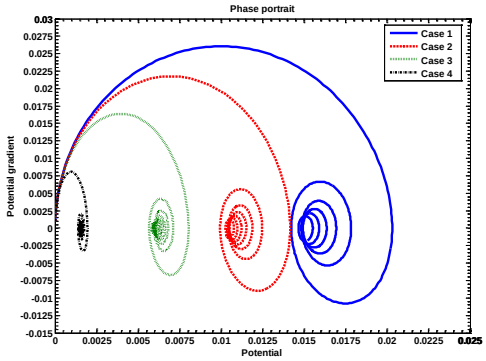

(c)

Fig. 7. Same as Figure (1). Various lines correspond to Case (1): $\mu = 1.15$ (blue line), Case (2): $\mu = 1.16$ (red line), Case (3): $\mu = 1.17$ (green line), and Case (4): $\mu = 1.18$ (black line), respectively. Different initial values used are $\eta_i = 0$, $\left(\eta_\xi\right)_i = 10^{-3}$, and $\left(\eta_{\xi\xi}\right)_i = 10^{-3}$. The other input parameters kept constant are $M_o = 10^{-8}$, $\in_T = 0.4$, $T = 65$, and $\left(\lambda_{De}/\lambda_J\right) = 10^{-20}$.

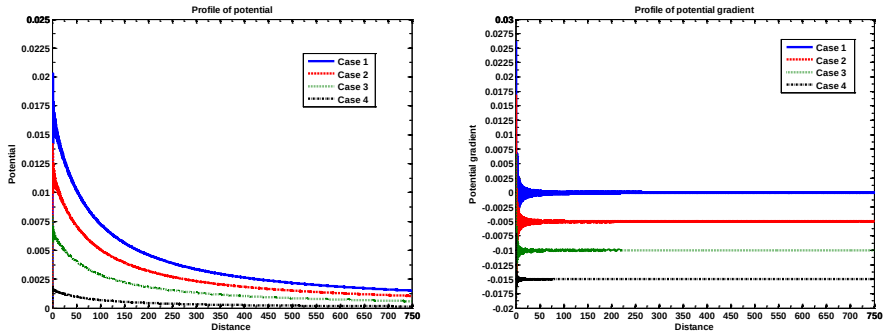

(a) (b)

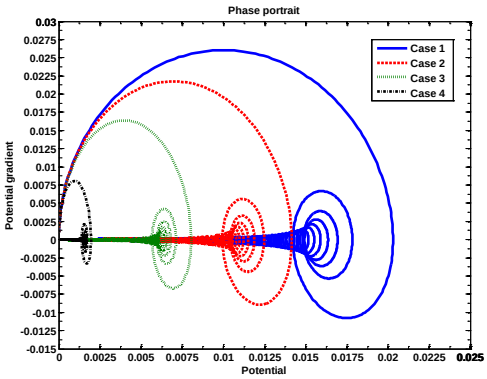

(c)

Fig. 8. Same as Figure (7), but on the unbounded scale.